PROCEEDINGS, 48th Workshop on Geothermal Reservoir Engineering
Stanford University, Stanford, California, February 6-8, 2023
SGP-TR-224

An Improved Reactive Transport Model for Supercritical Geothermal Systems

Tianfu Xu, Guanhong Feng, and Ye Gong

Key Laboratory of Groundwater Resources and Environment, Ministry of Education, Jilin University, Changchun, 130021, China

Tianfu_Xu@jlu.edu.cn

Keywords: Supercritical geothermal; Reactive transport modeling; Code development; Quartz

ABSTRACT

Subsurface reactive transport modeling (RTM) is an effective approach for studying the fundamental of earth sciences, widely applied in geo-resources development and contamination remediation, etc. In the traditional RTM, the temperature upper limit is about 300ºC, which is not applicable for supercritical water conditions (greater than 374ºC, 22.1MPa). Because of the lack of a thermodynamic database for high-temperature conditions, the geochemical reactions are constrained in the aqueous phase in traditional RTM. Whereas, the chemical species can also be dissolved in the steam phase, particularly under supercritical conditions. In this study, we improved the existing reactive transport model, expanding its applicable scope towards supercritical geothermal conditions, based on the framework of TOUGHREACT. The IAPWS-IF97 formulation is implemented for calculating the properties of water in different phases. The database of Soltherm.xpt is introduced to extend the temperature upper limit, with a quaternary interpolation to consider the variation of the equilibrium constant (logK) with P/T conditions. A logK weighting method is proposed to describe geochemical reactions in both the steam, aqueous, and supercritical phases. Then, we applied the improved program to the Iceland IDDP field, to study the quartz dissolution/precipitation pattern during the formation of the supercritical geothermal reservoir, with the logK from Manning's formula. The results show that, since the intrusion emplacement, the quartz starts to dissolve along the edge of the magma body (300~400ºC isotherm). In the action of upward heat flux, the high-Si concentration area distributes more extensively above the intrusion.

1. INTRODUCTION

Supercritical fluids are potential ideal targets to promote geothermal energy development in the future (Reinsch et al., 2017). It is acknowledged that supercritical geothermal fluids refer to those under the temperature and pressure condition exceeding the water critical point (T_c=373.946 ℃, P_c=22.064 MPa). If the pressure in the fluid does not meet the demand, it is usually called superheated steam, which also has a high value of exploitation. Here we refer to them collectively as supercritical geothermal fluids. They feature high specific enthalpy and low viscosity, which are beneficial for heat extraction.

Reservoir's permeability is the key to the feasibility of geothermal development engineering, not only because it controls the injectivity and productivity during the operation, but it also determines the manner of heat transfer during the formation of the system, which influences system's development potential (Scott and Driesner 2018, Hayba and Ingebritsen 1997, Scott et al., 2015). Previous studies have revealed a transition around the permeability of 10^{-16} m^2, where the heat transfer manner transits between advection-dominated and conduction-dominated (Scott and Driesner 2018, Hayba and Ingebritsen 1997). It can be deduced that higher permeability implies higher injectivity and better heat recharge from surrounding rocks for future development. Hence, Scott et al. (2015) defined the supercritical geothermal resource stored in the formation of permeability higher than 10^{-16} m^2 as "exploitable". In addition, there are many studies showing that the dissolution/precipitation of minerals changes the porosity in geothermal reservoirs, especially during exploitation (Andre et al., 2006). Thus, understanding the evolution and distribution pattern of the permeability is critical for targeting a favorable reservoir for supercritical geothermal development. In the process of supercritical system formation, significant variations in temperature and pressure can cause an intensive dissolution and precipitation of the primary minerals, which considerably change porosity and permeability.

The common reactive transport modeling programs cannot meet the demand of supercritical conditions, because of two limitations. The first is the temperature upper limit of the thermodynamic database, usually 300ºC. The other is the solvent must be the aqueous phase, i.e., the solute transport and chemical reaction in the gaseous/supercritical conditions cannot be described. Therefore, we devote ourselves to developing the reactive transport simulation program that can satisfy supercritical conditions. In this paper, we introduce our ideas to address the limitation above. Then, a simplified application is presented to study quartz dissolution/precipitation patterns during the formation of a supercritical geothermal system.

2. CODE DEVELOPMENT

TOUGH2 is a general-purpose numerical simulation program for non-isothermal flows of multi-component, multiphase fluids in porous and fractured media (Pruess 1991, Pruess et al., 1999). Different equation-of-state (EOS) modules are developed for application in different geological scenarios, such as geothermal, CO_2 sequestration etc. TOUGHREACT (Xu et al., 2006, Xu et al., 2011a, b) is developed based on TOUGH2 with the extension of reactive transport modeling. The code has been applied to study extensively subsurface thermo-physical and geochemical processes. It can describe the interactions between minerals and fluids under local equilibrium or kinetics mechanisms, with coupling to solute transport in non-isothermal multiphase multi-component flow. The accuracy of this code has been well verified by substantial studies in different domains around the world.

We have developed an EOS module that can handle the supercritical conditions following Croucher and O'Sullivan (2008), Magnusdottir and Finsterle (2015), incorporating IAPWS-IF97 to calculate the physical and chemical properties of water under different phase conditions (Feng et al., 2021, Feng et al., 2022). The upper limits for pressure and temperature of IAPWS-IF97 are 100 MPa and 800°C, and when the pressure is below 50 MPa the temperature could reach up to 2000°C.

In TOUGH2, the items for the mass conservation equation are calculated by each phase and then assemble the matrix together. The phase transition is a challenge for any multiphase simulation program. Particularly for supercritical conditions, the phases involve liquid (water), gas (steam), and supercritical phase. In fact, the phase boundary between water and steam is the saturation line, while, there is no boundary between water/supercritical and steam/supercritical. Unlike the transition between water and steam, the transition from water (or steam) to supercritical is continuous without any gap. Hence, how to deal with the supercritical condition under the current calculation framework is significant, especially for the numerical continuity. Here, we propose to extend the saturation line, and artificially divide the supercritical phase into two parts, supercritical "gas" and supercritical "liquid", as shown in Figure 1. The iso-density contour line of critical density (322 kg/m^3) in the supercritical conditions is selected as the virtual extended saturation line, as the solid line in Figure 1. Thus, the system involving supercritical conditions could be treated as the regular liquid/gas two-phase system.

2.1 Temperature limit extension

As first proposed in our study (Feng et al., 2020), the thermodynamic database of aqueous species and minerals - Soltherm.xpt, developed by Reed and Palandri (https://pages.uoregon.edu/palandri/) was employed for TOUGHREACT. The same improvement has also been made in the current version TOUGHREACT v4.13. Not only the temperature but also the pressure dependence of equilibrium constants are considered. The P/T range extends up to 500MPa and 600°C. However, the solvent still must be the aqueous phase, where the chemical reactions occur. The critical density of water is 322 kg/m^3, thus, the logK in the database is restricted to the P/T condition with water density higher than 350 kg/m^3, while the logK with lower density is omitted, as shown in Figure 1. Within the present framework of TOUGHREACT, the logK data could be read through two methods, values at different temperature points or regression equations coefficients, among which, the latter one possesses a higher priority. If the regression coefficients are absent, they would be calculated from the equilibrium constants at given temperatures.

In Soltherm.xpt, the equilibrium constants are arranged as tabular values at different P/T values. In this code development work, we adopt this data-reading method, and the logK data at different temperatures are calculated by quaternary interpolation. Only some minor modifications are made to the Soltherm.xpt database and the subroutine program of file input. Nothing is changed on other input files.

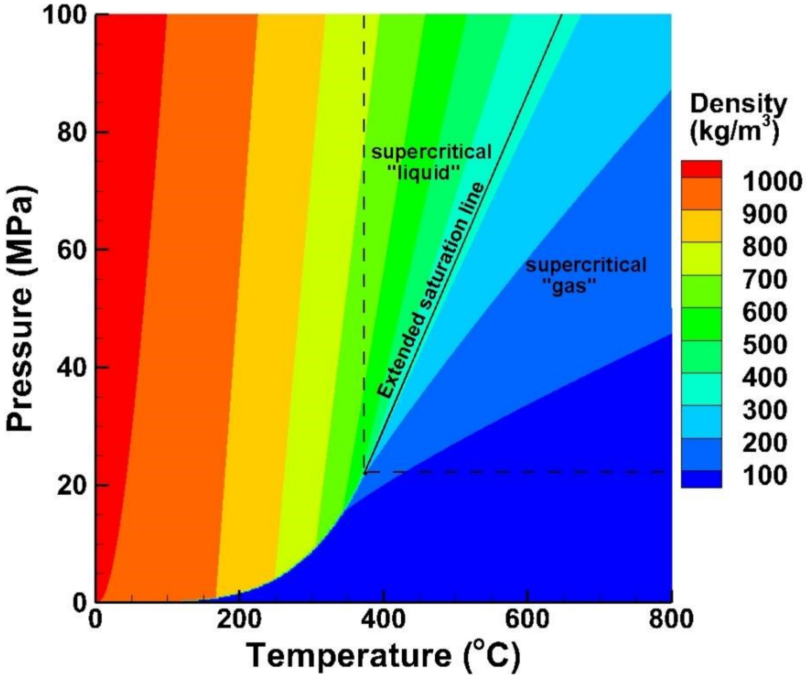

Figure 1: Water density distribution and applicable range for the thermodynamic database Soltherm.xpt.

2.2 Chemical reactions in the gaseous/supercritical phase

Although the temperature limit of logK has been extended up to 600°C, it still cannot deal with the reactive transport process under supercritical conditions because of the lack of data under steam and supercritical state. Even if the data is obtained, within the current reactive transport modeling framework, the solute transport of primary species and chemical reactions are constrained in aqueous phases, and the pertinent geochemical behavior in steam and supercritical phases are neglected, some further code development work is needed.

This code development work is based on the framework of TOUGHREACT. There are two approaches to realizing the description of reactive transport in all phases. The first is to calculate it separately, i.e., the reactive transport processes are calculated for each phase respectively, and the other is to calculate it integrally as a whole phase.

For a system containing large amounts of species, calculating separately is a more feasible way. The only problem is the calculation of the geochemical reaction needs to be repeated in phases. Each phase needs a set of primary variables. The mineral dissolution/precipitation needs to calculate by each phase and sum them up.

There is little data on the logK under the steam and supercritical conditions. Because there is no hydrolysis for quartz, there are some studies on the logK data of quartz under those conditions, such as Manning (1994), as shown in Figure 2 and Equ (1). In this study, we incorporate the formula of Manning into TOUGHREACT to explore the geochemical behavior of quartz during the formation process of a supercritical geothermal system.

$$\log K = 4.262 - \frac{5764.2}{T} + \frac{1.7513\times10^6}{T^2} - \frac{2.2869\times10^8}{T^3} + \left[2.8454 - \frac{1006.9}{T} + \frac{3.5689\times10^5}{T^2}\right]\log \rho_{\mathrm{H_2O}} \tag{1}$$

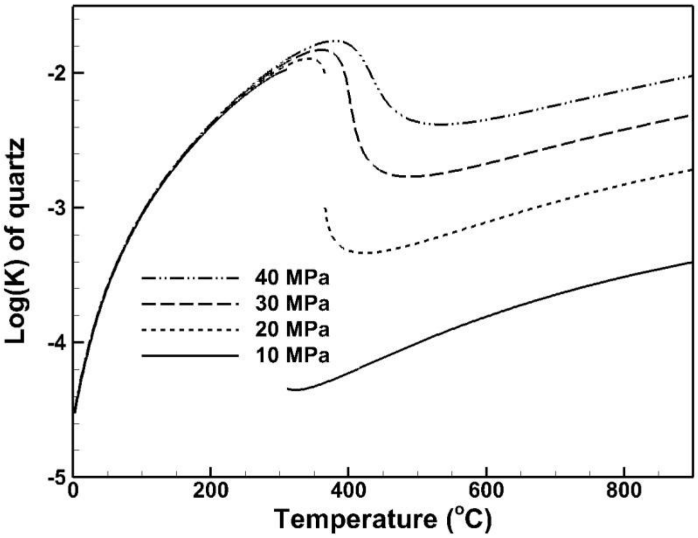

Figure 2: Quartz solubility variation with the temperature at different pressures in pure water

Here, we adopt the approach to calculate it integrally as a whole phase. Due to different Darcy's velocities and equilibrium constants in different phases, the mixture velocity for solute transport and equilibrium constant for geochemical reaction needs to be weighted by phase properties. As discussed above, the equilibrium constant is equal to the activity of dissolved SiO_2 in the unit of mol/kg water. Then the mixture equilibrium constant (K) could be expressed as Equ (2), where ρ is the mixture density.

$$K\rho = K_G\rho_G + K_L\rho_L \tag{2}$$

In TOUGHREACT, the implicit differential equation for reactive solute transport was written as Equ (3), where only the species concentration in the aqueous phases is considered. In this study, besides the aqueous phase, gaseous and supercritical phases are also potential solvents for quartz, in which the reactive transport process can occur.

$$S_{l,n}^{k+1}\phi_n^{k+1}c_n^{k+1} - S_{l,n}^{k}\phi_n^{k}c_n^{k} = \frac{\Delta t}{V_n}\sum_m A_{nm}\left[(\varepsilon_{nm}c_n^{k+1} + (1-\varepsilon_{nm})c_m^{k+1})v_{nm}^{k+1} + D_{nm}\frac{c_m^{k+1}-c_n^{k+1}}{d_{nm}}\right] + r_n^{k+1}\Delta t + q_n^{k+1}\Delta t \tag{3}$$

$$\phi_n^{k+1}c_n^{k+1} - \phi_n^{k}c_n^{k} = \frac{\Delta t}{V_n}\sum_m A_{nm}\left[\left(\varepsilon_{nm}c_{n,G}^{k+1} + (1-\varepsilon_{nm})c_{m,G}^{k+1}\right)v_{nm,G}^{k+1} + D_{nm}\frac{c_{m,G}^{k+1}-c_{n,G}^{k+1}}{d_{nm}} + \left(\varepsilon_{nm}c_{n,L}^{k+1} + (1-\varepsilon_{nm})c_{m,L}^{k+1}\right)v_{nm,L}^{k+1} + D_{nm}\frac{c_{m,L}^{k+1}-c_{n,L}^{k+1}}{d_{nm}}\right] + r_n^{k+1}\Delta t + q_n^{k+1}\Delta t \tag{4}$$

Thus, the improved differential equation for solute transport could be written as Equ (4), where, the $C_{n,G}$, $C_{n,L}$ and C_n are the dissolved SiO_2 volumetric concentration in the gaseous, aqueous phase, and the saturation-weighted value, as Equ (5). Then, we can obtain, for SiO_2 saturated fluid, the volumetric concentration in each phase, $C_{n,G}$, $C_{n,L}$ equals to the product of equilibrium constant $K_{n,G}$, $K_{n,L}$ with fluid density ρ_G, ρ_L of each phase. While for unsaturated fluid, it is assumed that the concentration per unit mass in different phases positively relates to the equilibrium constant, as Equ (6).

$$S_G C_{n,G} + S_L C_{n,L} = C_n \tag{5}$$

$$\frac{C_{n,G}/\rho_G}{C_{n,L}/\rho_L} = \frac{K_{n,G}}{K_{n,L}} \tag{6}$$

Thus, combining Equ (5) and (6), the SiO_2 concentration in each phase could be arranged as Equ (7) and (8) as a function of the weighted concentration.

$$C_{n,G} = \frac{1}{[1+S_L(\rho_L K_{n,L} - \rho_G K_{n,G})/\rho_G K_{n,G}]} \cdot C_n \tag{7}$$

$$C_{n,L} = \frac{1}{[1+S_G(\rho_G K_{n,G} - \rho_L K_{n,L})/\rho_L K_{n,L}]} \cdot C_n \tag{8}$$

Replace the $C_{n,G}$ and $C_{n,L}$ in Equ (4) with the expression in Equ (7) and (8), and then, we get the implicit differential expression of the solute transport equation for calculating the volumetric concentration of dissolved SiO_2.

3. APPLICATION EXAMPLE

3.1 Geological model

Following Scott and Driesner (2018), an X-Z two-dimensional model with a sphere-shaped magma chamber embedded is set up (shown in Figure 3) to obtain a general pattern of the dissolution/precipitation of quartz [4][25]. It is a simplification of IDDP-1 in Krafla, Iceland, which encountered magma at a depth of 2100m, with the magma chamber being about a sphere with a radius of 500 m[26-28]. This study focused on the evolutionary process of the supercritical hydrothermal system caused by the intrusion. Thus, we did not consider the intrusion process, and started the model after the emplacement of the magmatic body. The system extends from the ground surface to 5km in depth and 8km in width. The intrusion body was assumed to be at the center of the reservoirs with the major and the minor axis of 2km and 1km. The mesh of and above the intrusion body is further refined to better capture the detail of the hydrothermal flow.

The default porosity and permeability are set as 0.05 and 1mD. The rock matrix density, specific heat capacity, and thermal conductivity are 2700 kg/m^3, 1000 J/kg/°C, and 2.0 W/m/°C. The properties of the intrusion are set as the same as the formation. The brittle-ductile transition is considered. The permeability logarithmic linearly decreases from 1mD to 10^{-7}mD within the temperature range from 550°C to 750°C (i.e., T_{BDT} is 550°C~750°C). Thus, the intrusion is nearly impermeable initially. In this study, only when the temperature decreases below the T_{BDT}, the influence of quartz dissolution/precipitation on permeability is considered. Through the study, we found that due to the high reaction rate brought by high temperature, the results of the kinetics model make little difference from those of equilibrium model. Hence, the equilibrium mechanism is assumed to describe the quartz dissolution/precipitation.

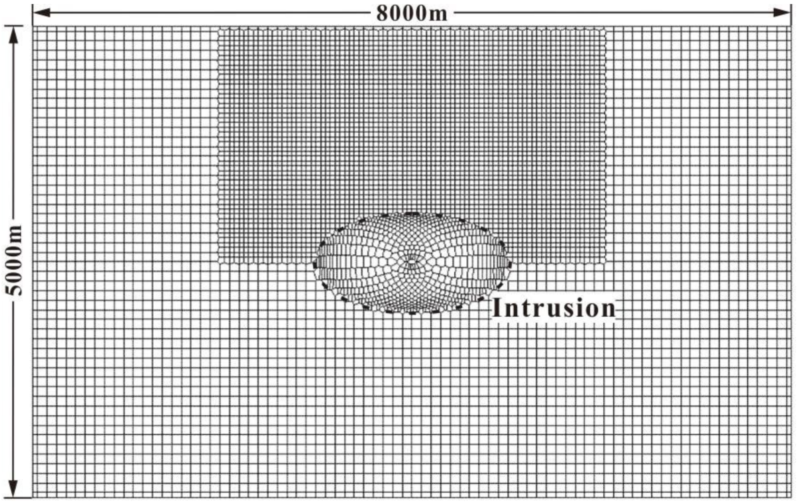

Figure 3: The conceptual model and mesh generation

The top boundary is the ground surface under the atmospheric condition with a temperature of 10°C and the bottom is recharged only by the terrestrial heat flux of 0.15 W/m^2 without fluid. It results in a geothermal gradient of 75°C/km with a thermal conductivity of 2.0 W/m/°C. The initial pressure distribution is hydrostatic, positively related to the depth and water density. The pressure and temperature at the reservoir bottom are 300°C and 45.9MPa. The intrusion body is assumed to emplace in the host rock instantaneously, with a temperature of 900°C and pressure of 50 MPa.

3.2 Results and discussion

Figure 4 demonstrates the distribution of dissolved SiO_2 at different times. The intrusion transfers heat and releases pressure, so the water around it is heated to the steam or supercritical phases. It can be seen that there are multi-plumes of heated fluid ascending above the intrusion body. The main quartz dissolution area lies in two distinct parts, the inner core and outer circular of the intrusion. As time goes on, the inner core shrinks, and the outer circle extends upward, particularly in the wings part. It shares a similar shape with the steam saturation distribution, as Figure 5b. The high-temperature steam is more likely to flow upward along the sides of the intrusion, forming the boiling zone, with the cold dense water flowing downward. This is because the downward flow of liquid water directly above the intrusion hampers the upward transfer of fluid and heat. While the liquid water along the intrusion’s two sides could flow through the further outer zone, forming a circulation. The two-phase fluid in the boiling zone and outer high-temperature liquid water comprises the high-concentration zone. After 2000 years, the high-concentration zone extends to the surface. And then, it becomes relatively smooth and uniform. The high-concentration part initially distributes at the two sides of the intrusion and moves towards the center as time goes on.

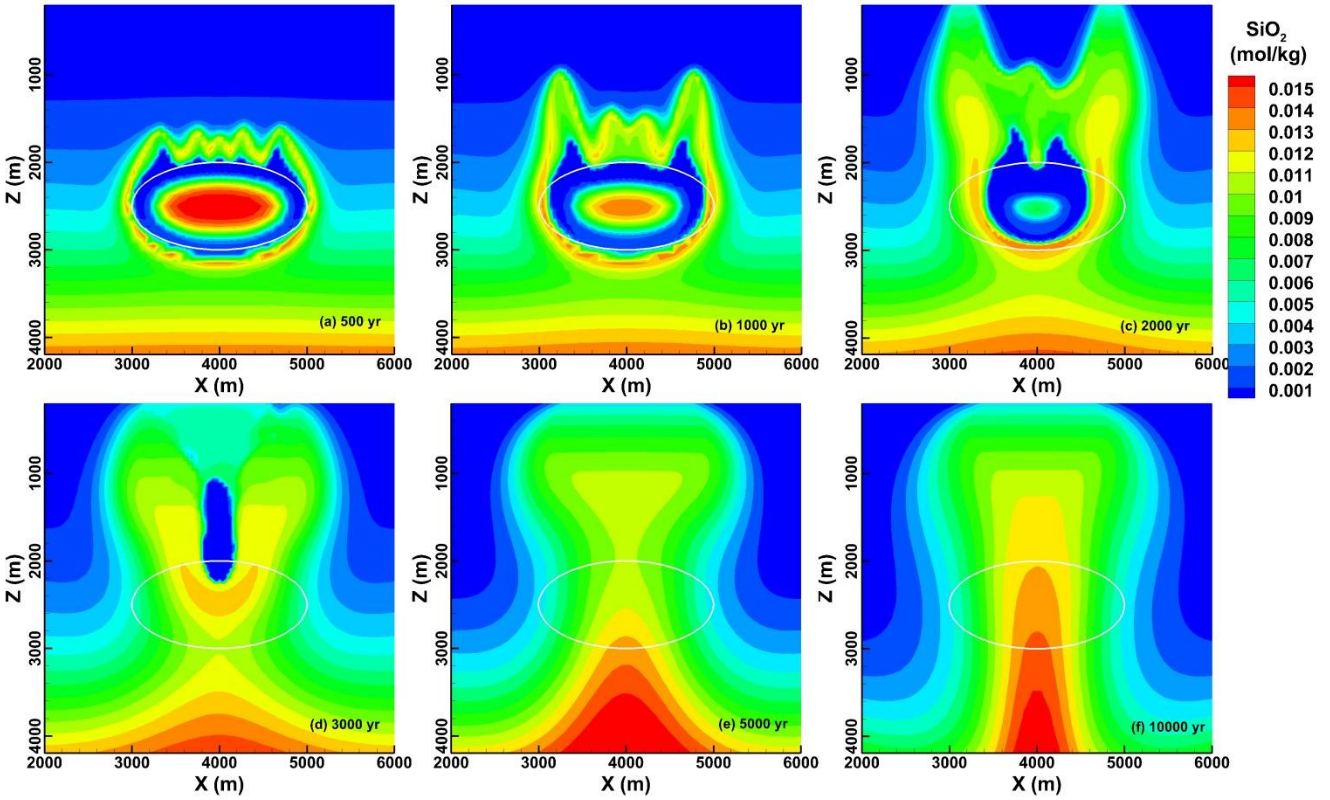

Figure 4: The dissolved SiO$_2$ concentration distribution at different times

The distributions of dissolved SiO$_2$ concentration, steam saturation, pressure, and temperature in the 1000th year are shown in Figure 5. The white circle in the center represents the scope of the intrusion. It could be seen that the fluid in the intrusion part remains steam. As in Figure 2, the solubility of quartz positively relates to temperature and pressure when the fluid presents in the state of steam phase. Not only the high temperature but also the high-pressure results in the “inner core” high-concentration part, while the concentration in the rest part of the steam phase is minimal. As a rather high P/T condition is given to the intrusion, the brittle-ductile transition makes the intrusion almost impermeable, and the heat transfer is accomplished mainly by conduction. The heat loss increases the fluid density and lowers the pressure. Hence, the variation trends and ranges of pressure and temperature are almost identical.

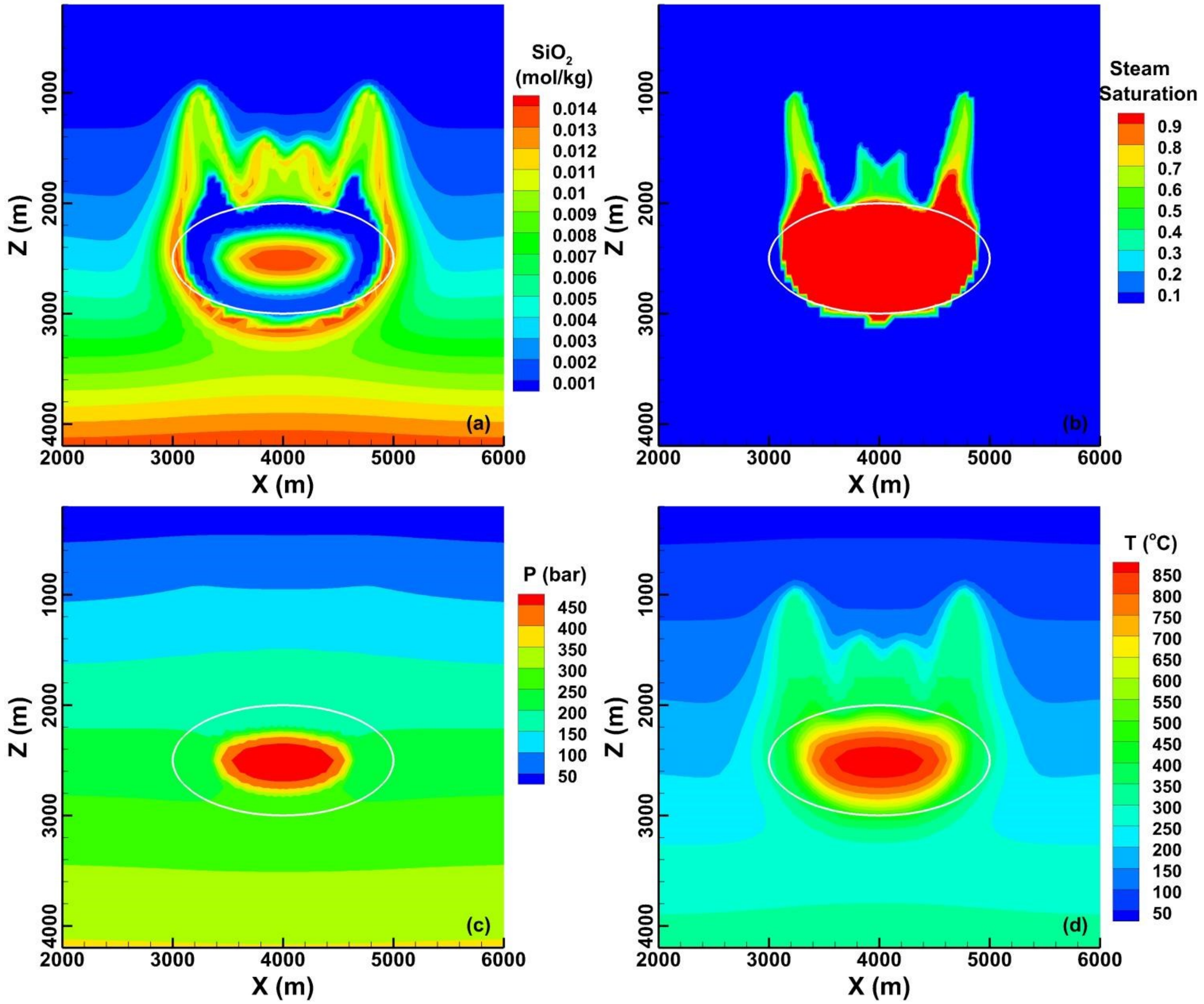

Figure 5: The distribution of (a) dissolved SiO_2 concentration, (b) steam saturation, (c) pressure and (d) temperature after 1000 years

The changes in quartz volumetric abundance are shown in Figure 6. During the whole process, the most significant changes occur around the intrusion body. The dissolution area appears on the two sides of the intrusion, while the precipitation area lies just above the intrusion. The maximum volumes of dissolution and precipitation could reach over 0.05% and 0.11%. It is worth noting that the quartz precipitates over a large area above the intrusion. At the same time, the concentration of dissolved SiO2 in this area increases compared to the initial. The porosity change induced by quartz dissolution/precipitations are shown in Figure 10, which strictly corresponds to the volumetric change. The general trend is to decrease, and the change is tiny, with a maximum of 2.2%.

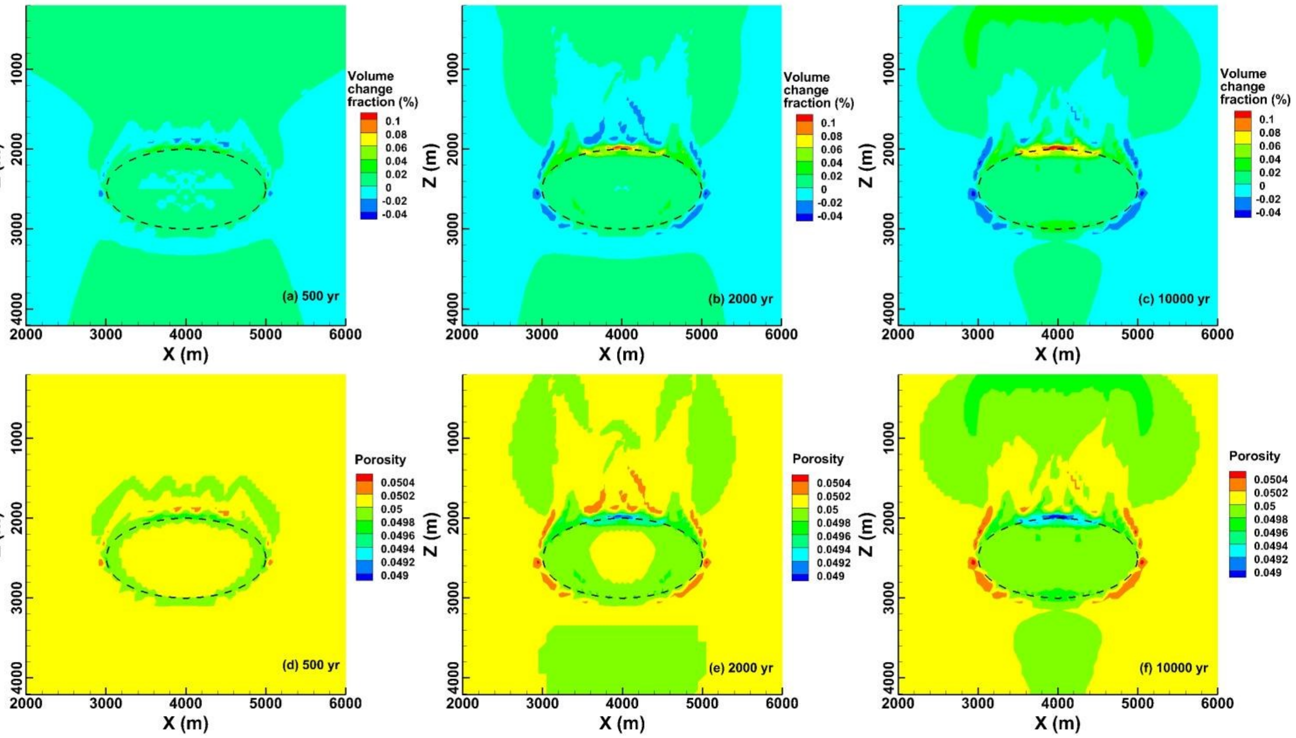

Figure 6: The distribution of changes in quartz volume fraction and porosity at different times

4. CONCLUSION

For the simulation study on the reactive transport process under supercritical conditions, we proposed two methods to enhance the current RTM program capability, and then we applied our program to study the dissolution/precipitation patterns of quartz during the formation process of a supercritical geothermal system. Some conclusions could be drawn:

1) We introduced Soltherm.xpt to TOUGHREACT to extend the temperature upper limit of the thermodynamic database. Even though it cannot deal with actual supercritical conditions, but also meaningful for some studies on hydrothermal flow.

2) The greatest challenge is the lack of equilibrium constant data under steam and supercritical conditions. In addition, the reactive transport process in that conditions needs to be considered appropriately.

3) We describe the quartz geochemical behavior in different phases and found that the high-concentration zone of dissolved SiO_2 could be divided into two parts, the inner core and the outer circle. As time goes on, the inner core shrinks and the outer circle extends upward. The high-concentration part moves from the intrusion sides toward the center, and the concentration gets higher.

REFERENCES

Andre, L., Rabemanana, V., and Vuataz, F.: Influence of Water-rock Interactions on Fracture Permeability of the Deep Reservoir at Soultz-sous-Forets, France, Geothermics, 35, (2006), 507-531.

Croucher, A., O’ Sullivan, M.: Application of the Computer Code TOUGH2 to the Simulation of Supercritical Conditions in Geothermal Systems, Geothermics, 37, (2008) ,622 - 634

Feng, G., Xu, T., Wang, F., Wang, Y., Shi, Y.: Modeling Analyses of Fluid Flow and Reactive Transport Processes for a Supercritical Geothermal System, Proceeding, World Geothermal Congress, 2020+1, Reykjavik, Iceland, (2021)

Feng, G., Wang, Y., Xu, T., Wang, F., and Shi, Y.: Multiphase Flow Modeling and Energy Extraction Performance for Supercritical Geothermal Systems, Renewable Energy, 173, (2021), 442-454.

Feng, G., Xu, T., Zhao, Y., and Gherardi, F.: Heat Mining From Super-hot Horizons of the Larderello Geothermal Field, Italy. Renewable Energy 197, (2022), 371-383.

Hayba, D., and Ingebritsen, S.: Multiphase Groundwater Flow near Cooling Plutons. Journal of Geophysical Research: Solid Earth, 102, (1997), 12235-12252.

Magnusdottir, L., and Finsterle, S.: An iTOUGH2 Equation-of-state Module for Modeling Supercritical Conditions in Geothermal Reservoirs, Geothermics, 57, (2015), 8 – 17,

Manning, C.: The Solubility of Quartz in H_2O in the Lower Crust and Upper Mantle, Geochimica et Cosmochimica Acta, 58, (1994), 4831-4839.

Pruess, K., TOUGH2: A General-purpose Numerical Simulator for Multiphase Fluid and Heat flow. Lawrence Berkeley Lab. Berkeley, Calif. (1991)

Pruess, K., Oldenburg, C., and Moridis, G.: TOUGH2 User's Guide, Version 2.0, Report LBNL-43134. Lawrence Berkeley National Laboratory, Berkeley, Calif. (1999)

Reinsch, T., Dobson, P., Asanuma, H., Huenges, E., Poletto, F., and Sanjuan, B.: Utilizing Supercritical Geothermal Systems: A Review of Past Ventures and Ongoing Research Activities, Geothermal Energy, 5 (2017), 16.

Scott, S., Driesner, T., and Weis, P.: Geologic Controls on Supercritical Geothermal Resources above Magmatic Intrusions, Nature Communications, 6, (2015), 7837

Scott, S., and Driesner, T.: Permeability Changes Resulting from Quartz Precipitation and Dissolution around Upper Crustal Intrusions. Geofluids, (2018), 1-19

Xu, T., Sonnenthal, E., Spycher, N., and Pruess, K.: TOUGHREACT - A Simulation Program for Non-isothermal Multiphase Reactive Geochemical Transport in Variably Saturated Geologic Media: Applications to Geothermal Injectivity and CO2 geological Sequestration, Computers & Geosciences 32, (2006), 145-165.

Xu, T., Spycher, N., Sonnenthal, E., Zhang, G., Zheng, L., and Pruess, K.: TOUGHREACT Version 2.0: A Simulator for Subsurface Reactive Transport under Non-isothermal Multiphase Flow Conditions. Computers & Geosciences 37, (2011), 763-774.

Xu, T., Spycher, N., Sonnenthal, E., Zheng, L., and Pruess, K.: TOUGHREACT User's Guide: A Simulation Program for Non-isothermal Multiphase Reactive Geochemical Transport in Variably Saturated Geologic Media, Version 2.0, Report LBNL-DRAFT. Lawrence Berkeley National Laboratory, Berkeley, Calif. (2012)